Polyhedron 33 (2012) 82–89

Contents lists available at SciVerse ScienceDirect

Polyhedron

journal homepage: www.elsevier.com/locate/poly

Three new pseudohalide bridged dinuclear Zn(II), Cd(II) complexes of pyrimidine derived Schiff base ligands: Synthesis, crystal structures and fluorescence studies

Sangita Ray [a], Saugata Konar [a], Atanu Jana [a], Sankar Jana [a], Amarendra Patra [a], Sudipta Chatterjee [b], James A. Golen [c], Arnold L. Rheingold [c], Sudhanshu Sekhar Mandal [a], Susanta Kumar Kar [a,*]

[a] Department of Chemistry, University College of Science, University of Calcutta, 92 A.P.C. Road, Kolkata 700009, India
[b] Department of Chemistry, Serampore College, Serampore, Hooghly 712201, India
[c] Department of Chemistry and Biochemistry, University of California, San Diego, CA 92093, USA

ARTICLE INFO

Article history:
Received 10 August 2011
Accepted 9 November 2011
Available online 6 December 2011

Keywords:
Zinc(II) and cadmium(II) complexes
Pyrimidine derived ligands
^{1}H NMR
X-ray crystal structures
Emission properties

ABSTRACT

One new dinuclear Zn(II) complex, $[(N_3)Zn(L_1)(\mu_{1,1}\text{-}N_3)]_2$ (**1**), and a dinuclear Cd(II) complex, $[(N_3)Cd(L_1)(\mu_{1,1}\text{-}N_3)]_2$ (**2**), of the potentially tridentate NNN-donor Schiff base ligand *N*-(4,6-dimethyl-pyrimidin-2-yl)-*N*′-(1-pyridin-2-yl-ethylidine)-hydrazine (L_1) and another dinuclear Cd(II) complex $[(NCS)Cd(L_2)(\mu_{1,3}\text{-}NCS)]_2$ (**3**) of a similar NNN donor Schiff base ligand, *N*-(4,6-dimethyl-pyrimidin-2-yl)-*N*′-pyridin-2-ylmethylene-hydrazine (L_2), have been synthesized and characterized by elemental analyses, IR, ^{1}H NMR, fluorescence spectroscopy and single crystal X-ray crystallography. The fluorescence spectral changes observed upon addition of the Zn(II) ion to a mixture of L_1 and azide showed high selectivity towards the Zn(II) ion over other metal ions. The ligands L_1 and L_2 are [1 + 1] condensation products of 2-hydrazino-4,6-dimethyl pyrimidine with 2-acetyl pyridine and pyridine-2-carbaldehyde, respectively. In the complexes **1** and **2** the two Zn(II) and Cd(II) centers are held together by $\mu_{1,1}$-bridged azide ions, while in **3** the two Cd(II) centers are bridged by $\mu_{1,3}$-thiocyanate ions. Complex **1** shows high chelation enhanced fluorescence compared to **2** and **3**. All the metal centers have a distorted octahedral geometry.

1. Introduction

The complexation of group 12 metal ions with polydentate Schiff base ligands is a well studied area of research in coordination chemistry [1–5]. These ligands have preparative accessibilities, structural variety and varied denticity, forming complexes of different coordination numbers and nuclearities with interesting molecular and crystalline architectures [6–16]. A substantial amount of work on pyridine and pyrazole derived Schiff base ligands have emerged in the literature, while works on pyrimidine derived Schiff base ligands are scarce. Pyrimidine derivatives play a dominant role in biological systems, the ring system being present in, for example, nucleic acids, several vitamins, co-enzymes and antibiotics [17–19]. Pyrimidine derivatives are also used in combination therapy with protease inhibitors to fight against HIV-1, the etiological agent of acquired immune deficiency syndrome [20,21]. Zn is an essential element in the biosystem. It is required in genetic materials, DNA, RNA polymerases, the regulatory Zn finger protein [structural motif for eukaryotic DNA-binding protein] in forming nucleic acids. The biological significance of Zn(II) has led to the development of numerous fluorescent chemo sensors [22]. The bioactivity of Cd is still in question, but unambiguously it is reported that the specific disease *itai itai* is caused by Cd poisoning [23,24].

As a sequel of our long standing interest in pyrimidine derived ligands [25–28] we have prepared tridentate NNN donor Schiff base ligands using 2-hydrazino-4,6-dimethyl pyrimidine and pyridine containing carbonyl compounds (2-acetyl pyridine and pyridine 2-carbaldehyde). Our interests are to observe the metal ion coordination environments and photoluminescence using 3*d*/4*d* metal ion templates, the organic ligands L_1 and L_2, and suitable bridging units. We choose zinc and cadmium because the d^{10} configuration in zinc permits a wide range of symmetries and various coordination numbers, i.e., 4, 5 or 6, relatively easily [29–31], while cadmium shows 4, 6, 7 coordination. Moreover, luminescent compounds are attracting much current research interest because of their many applications, including emitting materials for organic light emitting diodes, light harvesting materials for photo catalysis and fluorescent sensors for organic or inorganic analyses [32]. Introduction of electron-donating groups into the Zn(II) complexes enhances the quantum yield of the photoluminescence [33]. Hence it is important to understand the coordination chemistry and luminescence between group 12

---

* Corresponding author. Tel.: +91 033 23508386; fax: +91 033 23519755.
E-mail address: skkar_cu@yahoo.co.in (S.K. Kar).

0277-5387/$ - see front matter © 2011 Elsevier Ltd. All rights reserved.
doi:10.1016/j.poly.2011.11.031

metal ions for developing new materials which can function as fluorescent sensors [32]. In the present study (Scheme 1), using zinc perchlorate and cadmium perchlorate as the metal precursors, one new dinuclear zinc(II) complex $[(N_3)Zn(L_1)(\mu_{1,1}\text{-}N_3)]_2$ (**1**) and two new dinuclear cadmium(II) complexes, $[(N_3)Cd(L_1)(\mu_{1,1}\text{-}N_3)]_2$ (**2**) and $[(NCS)Cd(L_2)(\mu_{1,3}\text{-}NCS)]_2$ (**3**), have been synthesized with L_1 and L_2. We have reported the synthetic details, spectral characterizations, X-ray crystal structures and fluorescence studies of **1**, **2** and **3**, where pseudohalides act as terminal ligands as well as bridging ligands ($\mu_{1,1}$; $\mu_{1,3}$) in presence of the ligands L_1 and L_2.

2. Experimental

2.1. Materials

All chemicals were of reagent grade, purchased from commercial sources and used without further purification. 2-Acetyl pyridine, pyridine-2-carbaldehyde and methyl cyclohexane were purchased from the Aldrich Chemical Company, USA and used without further purification.

Caution! Although we have not encountered any problems, it should be kept in mind that sodium azide and perchlorate compounds of metal ions are potentially explosive, especially in the presence of organic ligands. Only a small amount of the material should be prepared and it should be handled with care.

2.2. Physical measurements

The infrared spectra of the complexes were recorded on a Perkin-Elmer RX I FT-IR spectrophotometer with KBr discs (4000–300 cm^{-1}). Elemental analyses (C, H and N) were carried out using a Perkin-Elmer 2400 II elemental analyzer. ^1H NMR spectra were recorded on a Bruker 300 MHz FT-NMR spectrometer using trimethylsilane as an internal standard in d_6-DMSO for complexes **1**, **2** and **3**. Steady state absorption and fluorescence spectra for all three complexes and the Schiff base ligands were measured with a Hitachi UV–Vis U-3501 spectrophotometer and a Perkin-Elmer LS50B fluorimeter, respectively, at room temperature (298 K). All the spectral measurements were done at $\sim 10^{-5}$ to 10^{-6} (M) concentration of solute in order to avoid aggregation and self-quenching.

Fluorescence quantum yields of the zinc and cadmium pseudohalide complexes of the ligands were calculated using β-naphthol as the reference with a known Φ_f (0.23) in MCH solvent, using the following equation [34,35]

$$\Phi_f = \Phi_f^0 \frac{n_f^2 A \int I_f^0(\lambda_f) d\lambda_f}{n_{0f}^2 A^0 \int I_f(\lambda_f) d\lambda_f}$$

Here n_0 and n are the refractive indices of the solvents, A^0 and A are the absorbance's, Φ_f^0 and Φ_f are the quantum yields, and the integrals denote the area of the fluorescence band for the standard and the sample, respectively.

2.3. Syntheses of the ligands (L_1 and L_2)

The ligand L_1 was synthesized by refluxing a methanol solution (30 ml) of 2-hydrazino-4,6-dimethyl pyrimidine [36,37] (1.38 g, 10 mmol) with 2-acetyl pyridine (1.21 g, 10 mmol) taken in the same solvent. The refluxing was continued for 1 h at water bath temperature. The resulting light yellow solution was filtered and kept at room temperature for slow evaporation. A light yellow microcrystalline compound separated after a week. It was filtered

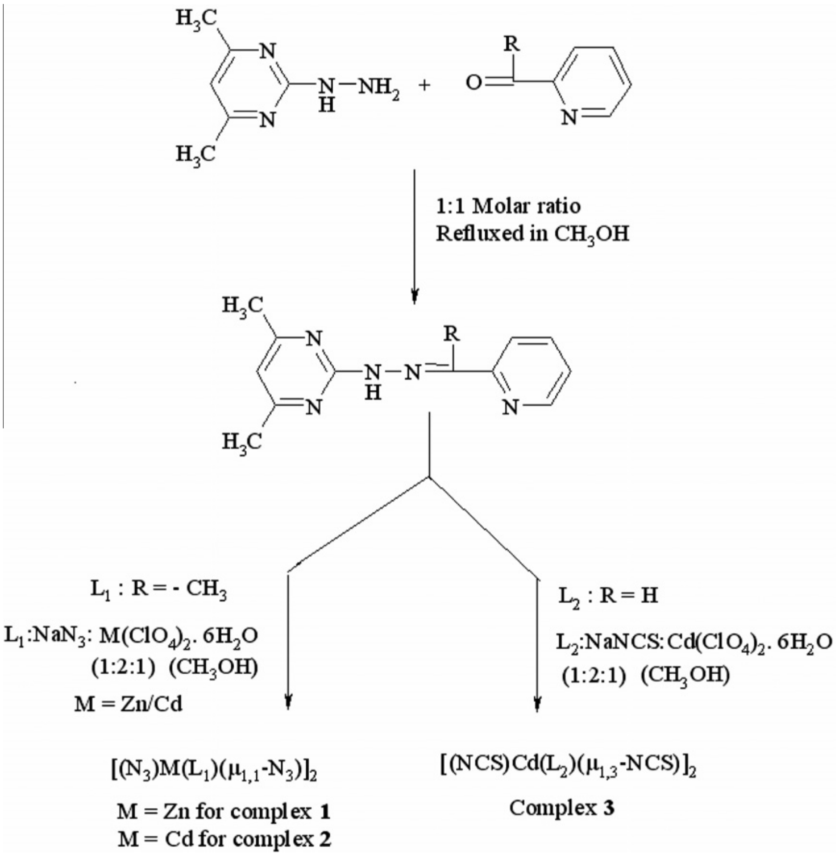

Scheme 1.

off, washed several times with cold methanol and dried in vacuo over fused $CaCl_2$.

L_1: Yield: 2.10 g (81%); mp (°C) 140. *Anal.* Calc. for $C_{13}H_{15}N_5$: C, 64.73; H, 6.22; N, 29.04. Found: C, 64.55; H, 6.15; N, 28.82%; IR (KBr, ν/cm^{-1}): 3270 (m) ($\nu_{N–H}$), 2980 (w), 2920 (w) ($\nu_{C–H}$), 1360 (s) (δ_{CH_3}), 1215 (ms) ($\nu_{C=C}$), 1065 (m) (pym), 1640 ($\nu_{C=Npym}$), 1635 ($\nu_{C=NH}$); ^{1}H NMR (d_6-DMSO, δ/ppm): 2.46 (6H, s, 4′-CH_3 and 6′-CH3), 2.52 (3H, s, =C–CH_3), 6.81 (1H, s, H-5′), 7.46 (1H, t, 7.8 Hz, H-4), 7.94 (1H, br d, 8.1 Hz, H-3), 8.69 (1H, dd, 4.0, 0.8 Hz, H-6), 10.23 (1H, br s, NH).

The ligand L_2 was prepared following the same procedure as that of L_1, but using pyridine-2-carbaldehyde (2.40 g, 10 mmol) in place of 2-acetyl pyridine.

L_2: Yield: 3.13 g (85%); mp (°C) 152. *Anal.* Calc. for $C_{12}H_{13}N_5$: C, 63.43; H, 5.72; N, 30.83 Found: C, 63.22; H, 5.61; N, 30.20%; IR (KBr, ν/cm^{-1}): 3265 (m) ($\nu_{N–H}$), 2975 ($\nu_{C–H}$), 1590 (mbr) (pym), 1570 ($\nu_{C=NPy}$), 1640 ($\nu_{C=Npym}$), 1630 ($\nu_{C=NH}$); ^{1}H NMR (d_6-DMSO, δ/ppm): 2.46 (6H, s, 4′-CH_3 and 6′-CH3), 6.79 (1H, s, H-5′), 7.46 (1H, dd, 7.8, 4.5 Hz, H-5), 7.96 (1H, t, 7.8 Hz, H-4), 8.13 (1H, br d, 8.1 Hz, H-3), 8.3 (1H, s, =C–H), 8.69 (1H, dd, 4.5 Hz, H-6), 11.54 (1H, br s, NH).

2.4. Preparation of the complexes

2.4.1. Preparation of complex **1**

To a methanol solution (30 ml) of $Zn(ClO_4)_2·6H_2O$ (0.744 g, 2 mmol), a solution of the Schiff base L_1 in the same solvent (0.482 g, 2 mmol) was slowly added, followed by a solution of sodium azide (0.260 g, 4 mmol) in a minimum volume of aqueous methanol with constant stirring. The stirring was continued for additional 2 h and filtered. The light yellow solution was kept at room temperature, which produced yellow hexagonal crystals suitable for X-ray diffraction after 10 days. The crystals were isolated by filtration and air-dried. Yield: (0.395 g, 61% with respect to zinc). *Anal.* Calc. for $C_{26}H_{30}N_{22}Zn_2$: C, 40.06; H, 3.59; N, 39.53. Found: C, 40.01; H, 3.51; N, 39.10%; IR (KBr, ν/cm^{-1}): 2054 (vs) (ν_{as}, N_3), 1579 (s) ($\nu_{C=Npym}$), 1630 ($\nu_{C=N}$); ^{1}H NMR (d_6-DMSO, δ/ppm): 2.41 (3H, d, 3.9 Hz, 4′-CH_3), 2.55 (3H, d, 3.9 Hz, 6′-CH_3), 2.58 (3H, s, =C–CH_3), 6.95 (1H, br s, H-5′), 7.65 (1H, br s, NH), 7.74 (1H, m, H-5), 8.09 (1H, br s, H-3), 8.18 (1H, br s, H-4), 8.50 (1H, br s, H-6).

2.4.2. Preparation of complex **2**

Complex **2** was prepared by the same procedure as **1** using $Cd(ClO_4)_2·6H_2O$ as the metal precursor. Yield: (0.548 g, 65.5%). *Anal.* Calc. for $C_{26}H_{30}N_{22}Cd_2$: C, 35.64; H, 3.42; N, 35.20. Found: C, 35.45; H, 3.39; N, 35.00%. IR (KBr, ν/cm^{-1}): 2058 (vs) (ν_{as}, N_3), 1575 (s) ($\nu_{C=Npym}$), 1625 ($\nu_{C=N}$); ^{1}H NMR (d_6-DMSO, δ/ppm): 2.39 (3H, s, 4′-CH_3), 2.46 (3H, s, 6′-CH_3), 2.50 (3H, s, =C–CH_3), 6.92 (1H, br s, H-5′), 7.66 (2H, br s, H-5 and NH), 8.05 (1H, br s, H-3), 8.15 (1H, br s, H-4), 8.53 (1H, br s, H-6).

2.4.3. Preparation of complex **3**

To a methanol solution (30 ml) of $Cd(ClO_4)_2·6H_2O$ (0.838 g, 2 mmol), a solution of the Schiff base L_2 in the same solvent (0.454 g, 2 mmol) was slowly added with stirring at room temperature, followed by drop by drop addition of a 2 ml aqueous solution of KSCN (0.388 g, 4 mmol). The stirring was continued for an additional 2 h and the solution was then filtered. The pale yellow solution was kept at room temperature, which produced yellow hexagonal crystals suitable for X-ray diffraction after a week. The crystals were isolated by filtration and air-dried. Yield: (0.556 g, 61.5%). *Anal.* Calc. for $C_{28}H_{26}N_{14}S_4Cd_2$: C, 36.85; H, 2.85; N, 21.51. Found: C, 36.67; H, 2.80; N, 21.30%. IR (KBr, ν/cm^{-1}): 2098 (vs) and 2098 (vs) (ν_{as}, NCS), 1578 (s) ($\nu_{C=Npym}$), 1610 ($\nu^{C=N}$); ^{1}H NMR (d_6-DMSO, δ/ppm): 2.42 (3H, s, 4′-CH_3), 2.46 (s, 6′-CH_3), 6.94 (1H,

Table 1
Experimental data for crystallographic analysis of **1**, **2** and **3**.

Complex	**1**	**2**	**3**
Empirical formula	$C_{26}H_{30}N_{22}Zn_2$	$C_{26}H_{30}Cd_2N_{22}$	$C_{28}H_{26}Cd_2N_{14}S_4$
Formula weight	779.48	875.54	911.73
T (K)	150	100	293
Wavelength (Å)	0.71073	0.71073	0.71073
Crystal system	monoclinic	monoclinic	triclinic
Space group	*C*2/*c*	*C*2/*c*	$P\bar{1}$
Unit cell dimensions			
a (Å)	16.670(4)	16.927(4)	9.311(5)
b (Å)	14.544(3)	14.844(4)	13.761(5)
c (Å)	14.556(3)	14.249(4)	16.253(5)
α (°)	90	90	109.271(5)
β (°)	107.552(8)	104.876(3)	92.116(5)
γ (°)	90	90	104.893(5)
V (Å^3)	3364.8(13)	3460.3(16)	1882.8(14)
Z	4	4	2
D_{calc} (mg m^{-3})	1.539	1.681	1.608
Absorption coefficient (mm^{-1})	1.485	1.284	1.392
$F(000)$	1592	1744	904
θ range (°) for data collection	1.9–25.6	1.9–27.9	1.3–28.1
Index ranges	$-20 \leqslant h \leqslant 20$	$-21 \leqslant h \leqslant 22$	$-12 \leqslant h \leqslant 11$
	$-17 \leqslant k \leqslant 17$	$-19 \leqslant k \leqslant 18$	$-18 \leqslant k \leqslant 18$
	$-17 \leqslant l \leqslant 17$	$-11 \leqslant l \leqslant 18$	$-19 \leqslant l \leqslant 19$
Goodness-of-fit (GOF) on F^2	2.021	1.067	1.033
Completeness to θ = 25.00° (%)	98.7	97.2	93.8
Independent reflections [R_{int}]	3162 [R_{int} = 0.204]	3712 [R_{int} = 0.030]	8597 [R_{int} = 0.034]
Absorption correction	multi-scan	multi-scan	multi-scan
Refinement method	full-matrix least squares on F^2	full-matrix least squares on F^2	full-matrix least squares on F^2
Data/restraints/parameters	3162/0/229	3712/0/233	8597/442/0
Reflections collected	15358	12588	24938
Final R indices [$I > 2\sigma(I)$]	R_1 = 0.0442 wR_2 = 0.2240	R_1 = 0.0366 wR_2 = 0.0793	R_1 = 0.0439 wR_2 = 0.1225
Largest difference peak and hole (e Å^{-3})	0.87, −1.03	0.950, −0.481	−0.89, 1.03
Maximum and minimum transmission	0.832 and 0.793	0.9042 and 0.7833	0.8632 and 0.8446

Table 2
Selected bond distances (Å) and angles (°) in **1**, **2** and **3**.

Selected bonds	Value (Å)	Selected angles	(°)
*Complex **1***			
Zn1–N9	2.065(7)	Zn1–N9–Zn1A	103.5(3)
Zn1–N6	2.095(6)	N2–Zn1–N4	73.9(3)
Zn1–N4	2.160(7)	N2–Zn1–N5	146.8(3)
Zn1–N5	2.181(7)	N2–Zn1–N6	91.2(2)
Zn1–N9_a	2.424(7)	N2–Zn1–N9	114.7(2)
Zn1–N2	2.164(6)	N2–Zn1–N9_a	88.7(2)
		N4–Zn1–N5	72.9(3)
		N6–Zn1–N9	97.9(3)
*Complex **2***			
Cd1–N6 _a	2.461(3)	Cd1–N6–Cd1A	102.98(11)
Cd1–N1	2.319(3)	N1–Cd1–N4	69.18(10)
Cd1–N4	2.374(3)	N1–Cd1–N5	137.29(11)
Cd1–N5	2.353(3)	N1–Cd1–N6	89.01(10)
Cd1–N6	2.461(3)	N1–Cd1–N9	93.35(10)
		N1–Cd1–N6_a	121.22(10)
		N4–Cd1–N5	68.17(10)
		N4–Cd1–N6	82.25(9)
*Complex **3***			
Cd1–N11	2.337(5)	N11–Cd1–S2	92.59(11)
Cd1–S2	2.614(2)	N12–Cd2–S1	90.46(12)
Cd2–N12	2.287(5)	S2–Cd1–S3	83.54(5)
Cd2–S1	2.6611(19)	S2–Cd1–N1	98.49(10)
Cd1–S3	2.723(2)	S2–Cd1–N2	165.74(10)
Cd1–N1	2.374(4)	S2–Cd1–N5	125.08(10)
Cd1–N4	2.374(3)	N1–Cd1–N5	136.43(13)
Cd1–N5	2.353(3)	N1–Cd1–N11	90.58(14)
Cd1–N6	2.461(3)	N1–Cd1–N11	90.58(14)
Cd1–N2	2.348(4)	N2–Cd1–N5	67.88(13)
Cd1–N5	2.387(4)	N2–Cd1–N11	94.19(14)
		N5–Cd1–N11	86.98(14)
		S3–Cd1–N1	98.64(9)
		S3–Cd1–N2	91.55(10)
		S3–Cd1–N5	88.09(9)
		S3–Cd1–N11	170.43(12)

br s, H-5′), 7.66 (1H, br s, H-5), 7.91 (1H, br s, H-3), 8.11 (1H, br s, H-4), 8.22 (1H, br s, =C–H), 8.56 (1H, d, 4.5 Hz, H-6), 12.96 (1H, br s, NH).

3. Single crystal X-ray crystallography

Selected crystal data for **1**, **2** and **3** are given in Table 1 and selected metrical parameters of the complexes are given in Table 2. For complexes **1** and **3** data collections were made using a Bruker SMART APEX II CCD area detector equipped with a graphite monochromated Mo Kα radiation (λ = 0.71073 Å) source in the ω scan mode at 296(2) K. For complex **2** data collections were made using a CCD area detector equipped with a graphite monochromated Mo Kα radiation (λ = 0.71073 Å) source in the φ and ω scan mode at 208(2) K. Cell parameter refinement and data reduction were carried out using Bruker APEXII for complex **1** and Bruker SMART APEXII for complexes **1** and **3**. The structures of all the complexes were solved by conventional direct methods and refined by full-matrix least square methods using F^2 data. SHELXS-97 and SHELXL-97 programs [38] were used for the solution and refinement, respectively, of the structures of all the complexes.

4. Result and discussion

4.1. Syntheses

The ligands L_1 and L_2 were synthesized by the direct condensation reaction of 2-hydrazino-4,6-dimethyl pyrimidine with 2-acetyl pyridine and pyridine-2-carbaldehyde taken in methanol in a 1:1 mol proportion. Complexes **1**, **2** and **3** were obtained by mixing the ligands and the respective Zn(II) and Cd(II) salts and different pseudohalides taken in a 1:1:2 molar ratio in methanol. X-ray quality crystals of **1**, **2** and **3** were obtained upon slow evaporation of the suitable reaction mixtures at room temperature. Details are given in Section 2.

4.2. Structural description of complexes 1 and 2

A perspective view of complexes **1** and **2**, with the atomic numbering schemes, are shown in Figs. 1 and 2, respectively. Both complexes **1** and **2** crystallize in the space group *C*2/*c*. The structures of **1** and **2** consist of centrosymmetric $[Zn(L_1)(\mu_{1,1}\text{-}N_3)(N_3)]_2$

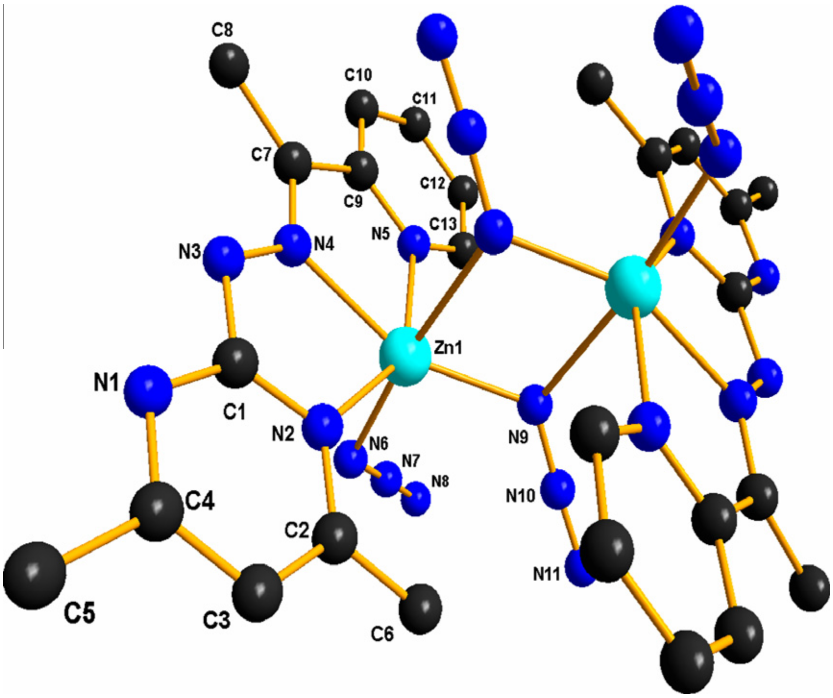

Fig. 1. Structural representation and atomic numbering scheme of **1** (H-atoms are omitted for clarity).

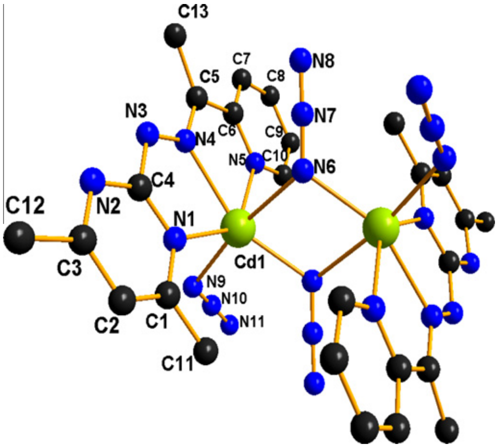

Fig. 2. Structural representation and atomic numbering scheme of **2** (H-atoms are omitted for clarity).

and $[Cd(L_1)(\mu_{1,1}-N_3)(N_3)]_2$ dimers, formed by the union of two $ZnL_1(N_3)_2$ and $CdL_1(N_3)_2$ fragments, respectively. The unit cells of **1** and **2** comprise of six molecules. Each zinc(II) and cadmium(II) cation shows a distorted octahedral geometry. In **1**, the equatorial plane is formed by N2 from pyrimidine, N4 from azomethine, N5 from pyridine and the N9 atom from the bridging azide group. In the case of **2**, N1 from pyrimidine, N4 from azomethine, N5 from pyridine and the N9 atom from a bridging azide form the equatorial plane. In both complexes the axial positions are occupied by a nitrogen atom from the bridging azide (N9A for **1**, N6A for **2**) and another nitrogen atom from a dangling azide (N6 for **1** and N9 for **2**). The Zn and Cd atoms are shifted by a distance of 0.246 and 0.269 Å downward from the equatorial plane towards the dangling azide unit, respectively. The Zn–N1, 1-azide bond distances of 2.059 and 2.420 Å are a little different from that of the Cd–N1, 1-azide bond distances of 2.461 and 2.270 Å, respectively. The N1, 1-azide–Zn–N1, 1-azide bond angle of 76.2° is smaller than the N1, 1-azide–Cd–N1, 1-azide bond angel of 77.02°. The existence of an inversion center causes the Zn1–N9–Zn1A–N9A and Cd1–N6–Cd1A–N6A units to form a parallelogram in each case (the sides and angles are $a = 2.42$ Å, $b = 2.065$ Å, 76.49° and 103.51° for **1**, $a = 102.98$ Å, $b = 77.02$ Å, 2.461° and 2.270° for **2**) In this dimeric unit, the Zn···Zn separation distance is 3.532 Å, which is smaller than the Cd···Cd separation distance of 3.704 Å. The bridging Zn1–N9–Zn1A angle of 103.51° is slightly larger than the bridging Cd1–N6–Cd1A angle of 102.98°. The crystal structure of this compounds can be described as a 1D layer due to intermolecular hydrogen bonding (Fig. 4). Both the complexes are stabilized by a network of intermolecular hydrogen bonding, H3A of N3 and N6 of the dangling azide for **1** and H1N of N3 and N9 of the dangling azide for **2** (Fig. 5). The details of the hydrogen bonding parameters are given in Table 3.

4.3. Structural description of complex 3

A perspective view of complex **3**, with the atomic numbering scheme, is shown in Fig. 3. Complex **3** crystallizes in the space group $P\bar{1}$. The structure of **3** consists of a dimer formed by two fragments, where CdL_2NCS units are bridged by two $\mu_{1,3}$-NCS anions in an equatorial axial bridging mode. Each cadmium center is attached to a dangling thiocyanate (Fig. 3). The unit cell comprises of two molecules. Here the ligand L_2 acts as a neutral tridentate NNN donor. Each Cd atom has a distorted octahedral geometry with a N_4S_2 chromophore. Three nitrogen atoms, N5 pyrimidine, N2 from azomethine, N1 from pyridine, and S2 from the bridging thiocyanate form the equatorial plane for Cd1, whilst N10 pyrimidine, N7 azomethine, N6 pyridine and S1 from another bridging thiocyanate form the equatorial plane for Cd2. The axial positions are occupied by N11 from a bridging thiocyanate and S3 from a dangling thiocyanate for Cd1, and those for Cd2, by N12 from a bridging thiocyanate and S4 from a dangling thiocyanate. Both the Cd atoms are shifted slightly towards the bridging thiocyanate, 0.042 Å for Cd1 and 0.025 Å for Cd 2. The Cd1–N11 and Cd1–S2 bond distances, 2.337 and 2.614 Å, are somewhat different to the Cd2–N12 and Cd2–S1 bond distances, 2.287 and 2.6611 Å, respectively and the N11–Cd1–S2 bond angle of 92.59° is larger than the N12–Cd2–S1 bond angle of 90.46°. In this dimeric unit, the Cd···Cd separation is 5.791 Å.

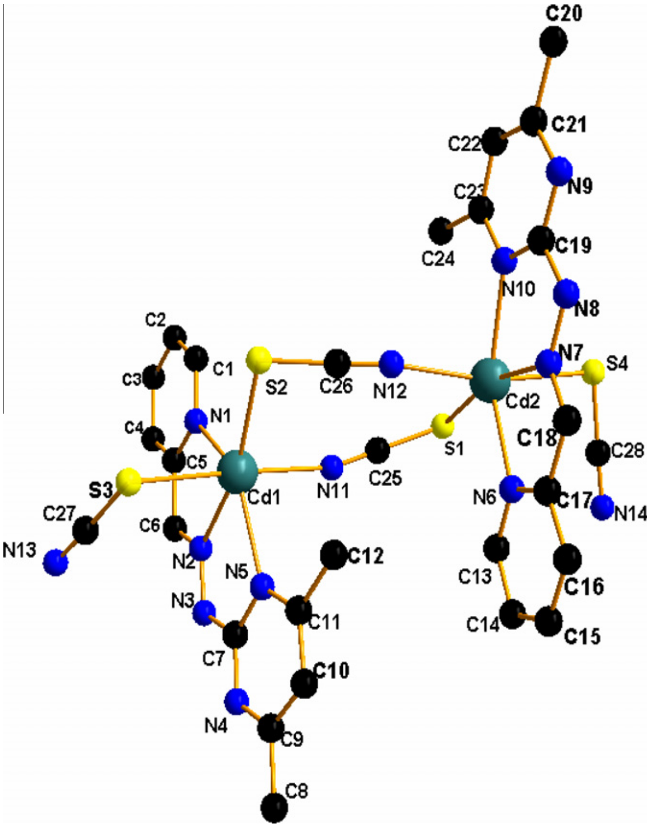

Fig. 3. Structural representation and atomic numbering scheme of **3** (H-atoms are omitted for clarity).

5. Characterization of the ligand and the complex species

5.1. ^{1}H NMR spectra

The structures of the ligands were secured from their 300 MHz ^{1}H NMR spectra in d_6-DMSO. The proton chemical shift assignments of the ligand L_2, received support from the observed coupling patterns and the coupling constants involved therein. The signal at δ 8.69 (1H, d, $J = 4.5$ Hz) in L_2 is typical of an α-proton resonance in a pyridine system with a low J_0 value and thus was assigned to H-6, which is coupled to H-5 (δ 7.46, 1H, dd, $J = 7.8$ and 4.5 Hz). The latter signal is coupled to a signal at δ 7.96 (1H, t, $J = 7.8$ Hz, H-4) which is in turn coupled to a resonance at δ 8.13 (1H, br d, $J = 8.1$ Hz) for H-3. A sharp singlet at δ 8.33 (1H) is in consonance with the presence of an azomethine proton, whilst that at δ 6.79 (1H, s) is in accord with the H-5 proton of the 4,6-dialkylpyrimidine unit. The appearance of two aromatic methyl's at the same position (δ 2.46, 6H, s) is in line with the presence of a symmetric

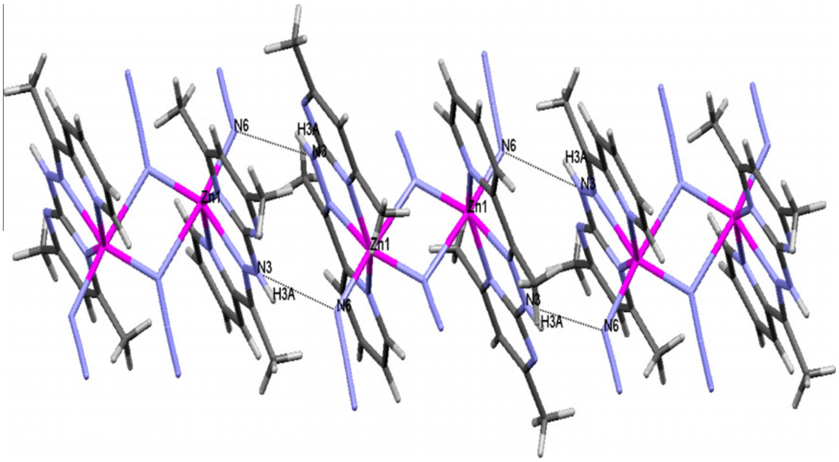

Fig. 4. Hydrogen bonding interactions in complex **1**.

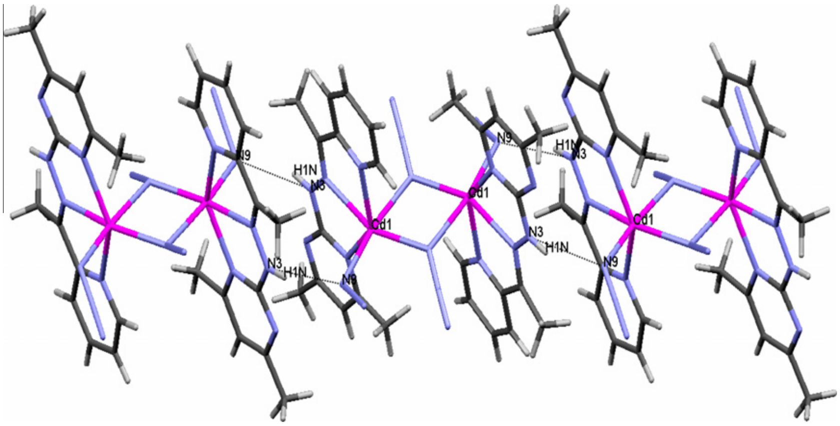

Fig. 5. Hydrogen bonding interactions in complex **2**.

Table 3
Details of hydrogen bond distances (Å) and angles (°) for **1** and **2**.

D–H···A	d(D–H)	d(H···A)	d(D···A)	<(DHA)
*Complex **1***				
N3–H3A···N6	0.8600	2.2200	2.897(9)	136.00
*Complex **2***				
N3–H1 N···N9	0.82(5)	2.19(5)	2.936(5)	152(5)

Symmetry transformations used to generate equivalent atoms:
For **1**: 3/2 − x, 1/2 − y, 2 − z.
For **2**: 3/2 − x, 1/2 − y, 1 − z.

pyrimidine unit. There is also a low field signal at δ 11.54 (1H, br s) for the arylhydrazone NH proton. The spectrum of the ligand L_1 is quite similar to that of L_2 but it lacks the signal for the azomethine proton, the place being taken by a vinyl methyl signal at 2.52 (3H, s) and corroborating the assigned structure of L_1.

In the complex (**3**) of L_2 there are six sets of signals for protons on sp^2 hybridized carbons, as in the parent ligand L_2, but the aromatic methyl groups are now non-equivalent because of the coordination with one pyrimidine nitrogen, and they consequently appear at different positions (δ 2.42 and 2.46, 3H each, br s). Similar observations were also made in the cases of the Cd and Zn complexes **2** and **1**, formed from L_1 and N_3.

It is noteworthy that solution phase ^{1}H NMR spectral studies of the complexes **1**–**3** indicated their similarity in the nature of coordination of L_1 and L_2, as appropriate, to Cd(II) and Zn(II). It was observed that H-3, H-6 and 4′-CH_3 experienced upfield shifts to the extent of 0.18–0.22, 0.13–0.18 and 0.04–0.07 ppm, respectively, while H-4, H-5 and H-5′ exhibited downfield shifts of about 0.15–0.24, 0.20–0.28 and 0.11–0.15 ppm, respectively.

5.2. Infrared spectroscopy

The infrared spectra of the complexes are consistent with the structural data given in this paper. The coordination mode of an azide is usually detected by an intense IR band due to $\nu_{as}(N_3)$ which occurs above 2000 cm^{-1}. In general, it appears above 2055 cm^{-1} for a $\mu_{1,1}$ bridging azide. The strong sharp bands at 2054 and 2058 cm^{-1} in the IR spectra of **1** and **2** are attributed to the presence of a $\mu_{1,1}$ bridging azide [39–42]. Complex **3** shows a strong band at 2125 cm^{-1} due to ν_{as}(NCS) of a $\mu_{1,3}$-NCS anion [43,44]. The strong $\nu_{C=N}$ azomethine bands occurring at 1630, 1625 and 1610 cm^{-1} for **1**, **2** and **3**, respectively, are shifted considerably towards lower frequencies compared to that of the free Schiff base ligands (1635 cm^{-1} for L_1 and 1630 cm^{-1} for L_2), indicating coordination of the imino nitrogen atom [46].

5.3. Emission behavior

The emission spectra of the Schiff base ligands (L_1 and L_2) and their Zn(II) and Cd(II) complexes (**1**, **2** and **3**) were recorded at

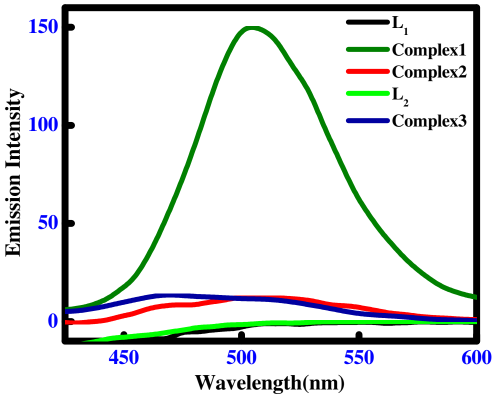

Fig. 6. Fluorescence emission properties of the free ligands, L_1 and L_2, and complexes **1**, **2** and **3**.

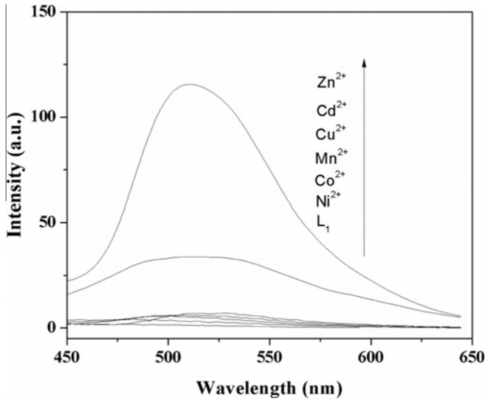

Fig. 7. Fluorescence emission (10^{-4} M) in the presence of Ni^{2+}, Co^{2+}, Mn^{2+}, Cu^{2+}, Cd^{2+} and Zn^{2+} (from bottom to top in CH_3OH).

room temperature (398 K) in methanol solvent on excitation of the corresponding absorption maxima of the ligand, and all the spectra are shown in Fig. 6. In the cases of both ligands, L_1 and L_2 have no such emission intensities but their metal complexes show enhanced fluorescence with emission maxima at ~505 nm for **1** and **2** and at 470 nm for complex **3**. The quenching of the emission intensity of the ligands probably is due to the occurrence of photoinduced electron transfer processes in the presence of a lone pairs of electrons of the donor atoms within the ligands [45]. The enhancement of the emission intensities of metal complexes may be due to the metal ligand chelation [46] or the increase in conformational rigidity of the ligands upon coordination [47]. The quenching of the emission intensity of a Schiff base ligand in the presence of transition metal ions is a common fact, but enhancement of fluorescence through complexation is, however, of much interest as it opens up the opportunity for photochemical applications of these complexes [48]. In the present study, the fluorescence spectra changes observed upon addition of various metal ions (Fe^{3+}, Co^{2+}, Ni^{2+}, Cu^{2+}, Hg^{2+} and Zn^{2+}) indicate that a 1:1 mixture of L_1 and azide in methanol show a high selectivity for Zn^{2+} (Fig. 7) compared to the other metal ions. Since the ligands have a too low emission intensity to calculate the quantum yield, we have only calculated quantum yields for the metal complexes **1**, **2** and **3** using β-naphthol in MCH Φ_f (0.23) as a secondary standard, and the results are shown in Table 4. From the quantum yield data in Table 4 it is clear that the quantum yields of the complexes increase with enhancement of the fluorescence intensity.

Table 4
Emission data and calculated quantum yields for complexes **1**–**3**.

Compound	Abs (λ_{max}) (nm)	Emission (λ_{em}) (nm)	Quantum yield (Φ) × 10^3
1	344	505	6.263
2	338	505	0.404
3	340	470	0.812

6. Conclusion

The pyrimidine derived NNN donor Schiff base ligands L_1 and L_2 form two dinuclear Zn(II) and Cd(II) complexes with L_1, and one Cd(II) complex with L_2, where the Zn and Cd centers are held by $\mu_{1,1}$ azide ions in **1** and **2**, and end-on bridged thiocyanate ions ($\mu_{1,3}$) bridging the Cd(II) centers in **3**. In all three complexes each metal center has a distorted octahedral geometry. The azide bridged complexes are isostructural. The ligands are fluorescent silent, but the Zn complex shows a strong chelation induced enhanced fluorescence compared to its Cd analogue. The fluorescence silent behavior of the ligands may probably be due to the presence of several non-bonding electron pairs on the nitrogen donors. These electrons are involved in coordinate bond formation with metal ions during complexation. The ligand n–π^* transitions are not allowed and the flexible bonds of the ligands cause the non-radiative channel to be active. During the metal binding process, non-radiative channels and flexible bonds are inactive due to strong binding. The Zn(II) ion, being harder than the Cd(II) ion, forms strong bonds with nitrogen donors. This strong binding of the ligand with Zn(II) may be the reason for its chelation enhanced fluorescence.

Acknowledgements

Sangita Ray acknowledges the University Grants Commission (UGC), New Delhi, India [Sanc. No. F. 5-1/2007(BSR)/5-16/2007(BSR), dated 12.02.2006] for a J.R.F. Financial support [Sanc. No. SR/S1/IC-27/2008, dated 13.03.2009] from the Department of Science & Technology (DST), New Delhi, India, is also gratefully acknowledged. X-ray crystallography was performed at the DST funded National Single Crystal Diffractometer facility at the Department of Chemistry, University of Calcutta.

Appendix A. Supplementary data

CCDC 817977, 817978 and 817979 contain the supplementary crystallographic data for **1, 2 and 3**. These data can be obtained free of charge via http://www.ccdc.cam.ac.uk/conts/retrieving.html, or from the Cambridge Crystallographic Data Centre, 12 Union Road, Cambridge CB2 1EZ, UK; fax: (+44) 1223-336-033; or e-mail: deposit@ccdc.cam.ac.uk.

References

[1] M.B. Davis, Coord. Chem. Rev. 164 (1997) 27.
[2] D.R. Smith, Coord. Chem. Rev. 172 (1998) 457.
[3] A.D. Garnovskii, A.L. Nivorozhkin, V.I. Minkin, Coord. Chem. Rev. 126 (1993) 1.
[4] V. Alexander, Chem. Rev. 95 (1995) 272.
[5] P.A. Vigato, S. Tamburini, L. Bertolo, Coord. Chem. Rev. 251 (2007) 1311.
[6] D. Braga, F. Grepioni, A.G. Orpen, Crystal Engineering: From Molecules and Crystals to Materials, vol. 538, Kluwer, Dordrecht, 1999. pp. 89–106.
[7] P. Comba, P.W. Hambley, Molecular Modelling of Inorganic and Coordination Compounds, second ed., VCH, Weinheim, 2001. pp. 161–162.
[8] K.-M. Dethlefs, P. Hobza, Chem. Rev. 100 (2000) 143.
[9] L. Brammer, Chem. Soc. Rev. 33 (2004) 476.
[10] C. Janiak, Coord. Chem. Rev. 250 (2006) 66.
[11] J.G. Planas, C. Masalles, R. Sillanpaa, R. Kivekas, F. Teixidor, C. Vinas, Cryst. Eng. Commun. 8 (2006) 75.

[12] M.K. Milčič, V.B. Medakovic, D.N. Sredojevic, N.O. Juranic, S.D. Zaric, Inorg. Chem. 45 (2006) 4755.
[13] M.J. Zaworotko, Cryst. Growth Des. 7 (2007) 4.
[14] G.A. Hembury, V.V. Borovkov, Y. Inoue, Chem. Rev. 108 (2008) 1.
[15] Q. Ye, D.-W. Fu, H. Tian, R.-G. Xiong, P.W.H. Chen, S.D. Huang, Inorg. Chem. 47 (2008) 772.
[16] X.-H. Chen, Q.-J. Wu, Z.-Y. Liang, C.-R. Zhan, J.-B. Liu, Acta Crystallogr., Sect. C 65 (2009) m190.
[17] W.G. Rice, J.A. Turpin, C.A. Schaeffer, L. Graham, D. Clanton, R.W. Buckheit Jr., D. Zaharevitz, M.F. Summers, A. Wallqvist, D.G. Covell, J. Med. Chem. 39 (1996) 3606.
[18] M. Otsuka, M. Fujita, Y. Sugiura, J. Med. Chem. 37 (1994) 4267.
[19] F. Zamora, M. Kunsman, M. Sabat, B. Lippart, Inorg. Chem. 36 (1997) 1583.
[20] M. Louloudi, Y. Deligiannakis, J.P. Tuchagues, B. Donnadien, N. Nadjiliadis, Inorg. Chem. 36 (1997) 6335.
[21] F. Jolibois, J. Cadet, A. Grand, R. Subra, N. Raga, V. Barone, J. Am. Chem. Soc. 120 (1998) 1864.
[22] E.L. Que, D.W. Domille, C.J. Chang, Chem. Rev. 108 (2008) 1517.
[23] J. Costamagna, J. Vargas, R. Latorre, A. Alvarado, G. Mena, Coord. Chem. Rev. 119 (1992) 67.
[24] Y.S. Sharma, H.N. Pandey, P. Mathur, Polyhedron 13 (1994) 3111.
[25] S. Gupta, S. Pal, A. Barik, A. Hazra, S. Roy, T.N. Mandal, S.M. Peng, G.H. Lee, M.S. El Fallah, J. Tercero, S.K. Kar, Polyhedron 27 (2008) 2519.
[26] S. Gupta, S. Pal, A.K. Barik, S. Roy, A. Hazra, T.N. Mandal, R.J. Butcher, S.K. Kar, Polyhedron 28 (2009) 711.
[27] S. Roy, T.N. Mandal, A.K. Barik, S. Pal, S. Gupta, A. Hazra, R.J. Butcher, A.D. Hunter, M. Zeller, S.K. Kar, Polyhedron 26 (2007) 2603.
[28] S. Roy, T.N. Mandal, A.K. Barik, S. Gupta, R.J. Butcher, M. Nethaji, S.K. Kar, Polyhedron 27 (2008) 593.
[29] R. Ghosh, S.H. Rahaman, C.-N. Lin, T.-H. Lu, B.K. Ghosh, Polyhedron 25 (2006) 3104.
[30] S. Sen, S. Mitra, P. Kundu, M.K. Saha, C. Krüger, J. Bruckmann, Polyhedron 16 (1997) 2475.
[31] H. Sigel (Ed.), Metal Ions in Biological Systems, vol. 10, Dekker, New York, Basel, 1979.
[32] L.D.L. Durantaye, T. McCormick, X.-Y. Liu, S. Wang, Dalton Trans. (2006) 5675.
[33] H.-C. Lin, C.-C. Huang, C.-H. Shi, Y.-H. Liao, C.-C. Chen, Y.-C. Lin, Y.-H. Liu, Dalton Trans. (2007) 781.
[34] S. Jana, S. Ghosh, S. Dalapati, N. Guchhait, Spectrochim. Acta, Part A 78 (2011) 463.
[35] R.B. Singh, S. Mahanta, S. Kar, N. Guchhait, Chem. Phys. 342 (2007) 33.
[36] G.M. Kosolapoff, C.H. Roy, J. Org. Chem. 26 (1961) 1895.
[37] M.P.V. Boarland, J.F.W. McOmie, R.N. Timms, J. Chem. Soc. (1952) 4691.
[38] G.M. Sheldrick, Programs for the Solution and Refinement of Crystal Structures, SHELXTL version 5.1., Bruker AXS P4 Inc., Madison, WI, USA, 1999.
[39] G.A. van Albada, M.T. Lakin, N. Veldman, A.L. Spek, J. Reedijk, Inorg. Chem. 34 (1995) 4910.
[40] E. Ruiz, J. Cano, S. Alvarez, P. Alemany, J. Am. Chem. Soc. 119 (1997) 1297.
[41] C. Adamo, V. Barone, A. Bencini, F. Totti, I. Ciofini, Inorg. Chem. 38 (1999) 1996.
[42] F. Fabrizi de Biani, E. Ruiz, J. Cano, J.J. Novoa, S. Alvarez, Inorg. Chem. 39 (2000) 3221.
[43] K. Nakamoto, Infrared and Raman Spectra of Inorganic and Coordination Compounds, fifth ed., Wiley, New York, 1997. pp. 59–60.
[44] S. Youngme, J. Phatchinkum, U. Suksangpanya, C. Pakawatchai, G.A.V. Albada, M. Quesada, J. Reedijk, Inorg. Chem. Commun. 9 (2006) 242.
[45] S. Basak, S. Sen, S. Banerjee, S. Mitra, G. Rosair, M.T.G. Rodriguez, Polyhedron 26 (2007) 5104.
[46] D.X. West, A.A. Nassar, Transition Met. Chem. 23 (1998) 321.
[47] S. Chattopadhyay, K. Bhar, S. Das, S. Satapathi, H.K. Fun, P. Mitra, B.K. Ghosh, Polyhedron 29 (2010) 2041.
[48] Y. Li, L. Shi, L.-X. Qin, L.-L. Qu, C. Jing, M. Lan, T.D. James, Y.-T. Long, Chem. Commun. 47 (2011) 4361.